



# ACOUSTICS 2012

## Diffraction-assisted rough ground effects

I. Bashir, S. Taherzadeh, T.J. Hill and K. Attenborough

The Open University, DDEM, Maths, Computing and Technology, Walton Hall, MK7 6AA  
Milton Keynes, UK  
i.bashir@open.ac.uk

Sound propagation over a smooth hard surface can be significantly altered by introducing roughness. For near grazing sound propagation over a smooth hard surface, the first destructive interference occurs at relatively high frequencies. However, the ground effect dips, corresponding to the first destructive interference, observed in Excess Attenuation (EA) spectra measured over rough surfaces, are at significantly lower frequencies. EA spectra over periodically- and randomly-spaced roughness elements with different cross-sectional profiles (semi-cylindrical, rectangular and wedge-shaped strips) are investigated. Periodic spacing results in multiple EA maxima, compared with the single broad EA maxima observed for random spacing. Roughness also causes surface waves. These surface waves are strongest near grazing incidence and their amplitudes and the frequencies at which they occur depend on the roughness height and mean centre-to-centre spacing. Numerical models such as Multiple Scattering Theory (MST) and the Boundary Element Method (BEM) are used to make predictions of the EA spectra which are compared with measurements. A semi-empirical effective impedance model for rough hard surfaces is developed and compared with data.

## 1 Introduction

When sound waves propagate over a rough hard surface at near grazing angles, it scatters both coherently and incoherently. For a point source and periodically distributed roughness, the scattered waves combine near grazing to form a reflected wave and a surface wave in addition to the direct wave.

$$P_{total} = P_{direct} + P_{refracted} + P_{surface}$$

The surface wave is an evanescent wave, which exists in the close vicinity of ground surface and is associated with an imaginary part (reactance) of the surface impedance that is greater than the real part (resistance).

Tolstoy's models [1,2] are derived from Biot [3] and Twersky [4, 5] theories by using a suitable boundary condition at smoothed boundary. Tolstoy [1, 2] formulated boss models for predicting scattering of sound from random surface roughness elements which are small compared to the incident wavelengths. These models predict that the effective impedance of a rough hard surface is purely imaginary but they over-predict the surface wave component found in experimental studies of the scattering of sound from surface roughness at near grazing angles [6]. Boulanger et al [7] modified Twersky's effective admittance model to generalize for arbitrary scatterer shape and proposed a heuristic method of introducing diffraction grating effects when sound propagates from a point source over periodically spaced surface roughness. Also Boulanger et al [8] have developed a model for acoustic scattering by a finite array of semi-cylinders embedded in a smooth hard surface using multiple scattering theory.

Since relatively little is known about the ground effect spectra that result from periodically-distributed roughness and the effects of roughness element shapes, systematic measurements have been made in an anechoic chamber of excess attenuation (EA) spectra due to a point source over variously shaped, periodically-spaced identical roughness configurations on an acoustically-hard boundary. The resulting data have been compared with data for randomly spaced identical elements and with numerical predictions. It is found that the influence of periodic spacing is to introduce additional ground effect dips related to the periodicity.

Section 2 describes the experimental procedures and laboratory arrangements. Section 3 presents measured Excess Attenuation (EA) data for random and periodically spaced roughness elements with various cross-sectional shapes. The three prediction methods (FEM, BEM and

MST) that have been used are summarized in section 4. Section 5 presents observed surface waves above roughness at near grazing angle. An effective impedance model is proposed and compared with data in section 6. Conclusions are drawn in section 7.

## 2 Measurement arrangements

Figure 1 shows a schematic of the experimental arrangement. A Tannoy driver fitted with a 1m long tube, of 3cm internal diameter was used as a point source and a Bruel & Kjaer type 4311 1/2-inch-diameter condenser microphone fitted with a preamplifier was used as a receiver. Both source and receiver were placed at a height of 0.07 m and at a horizontal separation of 0.7 m above a glass plate. A data acquisition system based on Maximum Length Sequence (MLS) was used for signal generation and signal processing. The background noise in the received microphone signals was removed by correlation with the known output sequence. The free field data needed for calculating excess attenuation spectra were obtained by raising source and receiver to a height of 2m above the grid floor of the anechoic chamber so that unwanted reflections were minimized. Measurements have been made of sound propagation over several small scale roughness configurations formed by placing strips of different cross-sectional shapes (semi cylindrical, triangular, short rectangular, tall rectangular and (approximately) square) with random or periodic spacing on the glass sheet. The strip locations were centred on the point of specular reflection which was halfway between source and receiver as they are at equal heights.

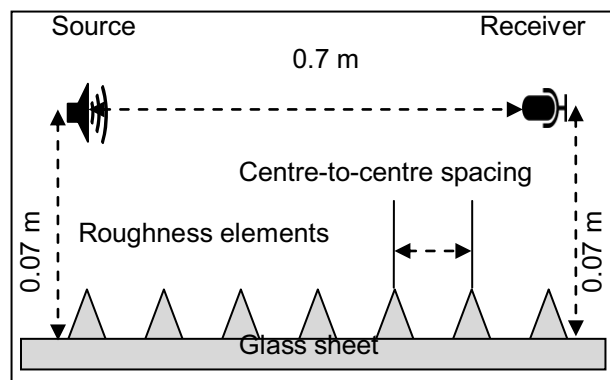


Figure 1: Schematic of the laboratory measurements of sound propagation over a rough surface.

### 3 Results

#### 3.1 Data for random spacing

Identical strips having different cross-sectional shapes were randomly spaced between source and receiver. For comparison with the corresponding periodic configurations, the spacings between the strips were normalized such that the sum of the separations divided by total number of strips was equal to the desired mean centre-to-centre spacing. To avoid overlapping roughness elements, a set of random numbers were generated with a mean value equal to the desired edge-to-edge distance (centre-to-centre spacing minus strip width). At each mean centre-to-centre spacing of between 3 and 8 cm five random distributions were tested.

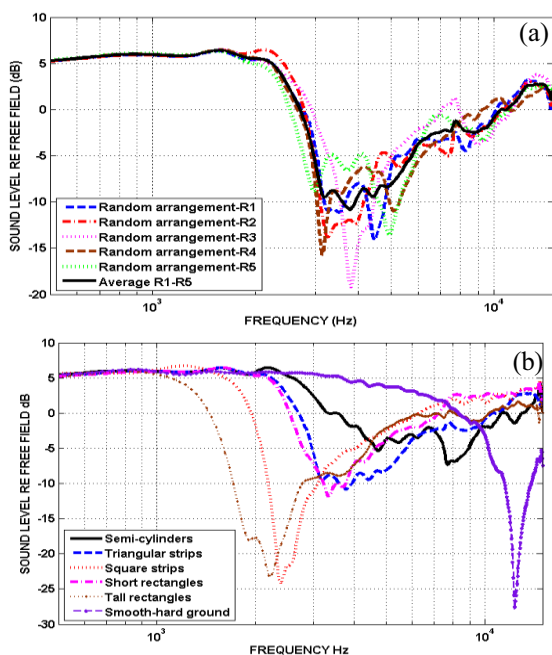


Figure 2: (a) Excess attenuation spectra measured over roughness elements randomly placed over glass sheet with mean centre-to-centre spacing of 0.05 m at source and receiver height of 0.07 m separated by 0.7 m (a) 15 triangular strips placed with five random distributions and their average (b) Averaged measured EA spectra over five random distributions of strips with surfaces composed of semi-cylinders, triangular strips, square strips, short rectangular strips or tall rectangular strips. The measured EA spectra for the smooth hard glass sheet (no roughness) are shown by the purple dotted (asterisk) curves.

Figure 2(a) compares the measured EA spectra for five different random distributions of 15 triangular strips with mean centre-to-centre spacing of 5 cm and the arithmetic mean spectrum. The averaging of the EA spectra reduces and broadens the ground effect dips due to each of the deterministic random distributions. Figure 2(b) show EA spectra measured over randomly-spaced strips with average centre-to-centre spacing of 5 cm. For the laboratory source-receiver geometry, the first destructive interference above a smooth hard ground would occur at a frequency of 12.3 kHz as shown by the EA spectrum obtained over for the glass plate (no roughness). In comparison the measured EA maxima in the presence of identical randomly spaced strips with various cross-sectional shapes (semi cylindrical, triangular, square, short rectangular and tall rectangular) are

at lower frequencies. Moreover they increase in magnitude and become sharper as the roughness height increases.

#### 3.2 Data for periodic spacing

Figure 3(a) shows excess attenuation (EA) spectra obtained over a glass sheet on which were placed odd numbers of semi-cylindrical strips (between one and fifteen) at a regular centre-to-centre spacing of 5 cm. In each case the strips were located symmetrically about the specular reflection point i.e. halfway between source and receiver since the source and receiver heights were equal. As the number of strips is increased, these show multiple distinct maxima compared with the single broad EA maxima observed for random spacing (see Fig.2). The frequency of the EA maximum shifts to lower frequencies as the number of strips increases.

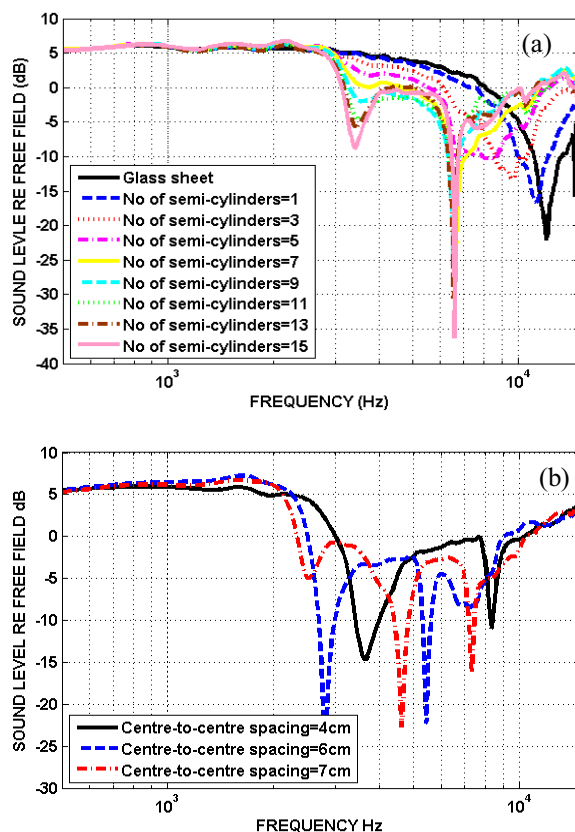


Figure 3(a): Measured excess attenuation spectra for source and receiver heights at 0.07 m separated by 0.7 m over (a) surfaces including between 3 and 15 semi-cylindrical strips with regular centre-to-centre spacing of 0.05 m (b) over surfaces including regularly-spaced triangular strips with centre-to-centre spacing of 0.04 m, 0.06 m and 0.07 m.

The measured EA spectra for regularly-spaced triangular strips in Figure 3(b) show two distinct EA maxima at 3.7 kHz and 8.4 kHz for a centre-to-centre spacing of 4cm (black solid line) which shift to lower frequencies as the centre-to-centre spacing is increased to 6cm (blue dash line). With a 6 cm centre-to-centre spacing there is some indication of a third EA maximum near 7 kHz. At a centre-to-centre spacing of 7cm (red dotted line) a third EA maximum shows clearly at 7.3 kHz while the other maxima move to even lower frequencies and that at the lowest frequency becomes relatively shallow. Similar behavior has been observed in the EA spectra obtained over

strips with other cross-sectional shapes (square, short and tall rectangles). The magnitude, number and frequency of occurrence of these multiple EA maxima vary with shape, cross-sectional area, height and centre-to-centre spacing. Consistently however increase in the centre-to-centre spacing between periodically spaced roughness elements moves the secondary (higher frequency) EA maxima to lower frequencies.

### 3.3 Discussion

#### 3.3.1 First EA maxima

The frequency of the first maxima (plotted as dips) observed in the EA spectra obtained over regularly-spaced roughness elements is similar to the main ground effect attenuation maximum (also shown as a dip) observed for random spacing of the same roughness elements. It is concluded that first EA maxima occur due to effectively finite impedance of rough hard ground and may be regarded as the *roughness-induced ground effect maximum*.

#### 3.3.2 Second EA maxima

The second EA maxima observed over periodically spaced roughness elements are influenced by the centre-to-centre spacing of the roughness elements. It is observed that, there is approximately a linear relationship between the wavelength at the second EA maximum and the centre-to-centre spacing. These correspond to inverse relationships with frequency and suggest that the frequency of the second EA maximum can be predicted from the spacing.

#### 3.3.3 Third EA maxima

The percentage of exposed surface between the strips plays an important part in determining the appearance of the third EA maxima. The third EA maximum has been observed when 50% or more of the ground surface is exposed i.e. the percentage roughness coverage is 50% or less. The 3<sup>rd</sup> EA maximum moves towards lower frequencies with increasing source and receiver height.

## 4 Comparison of data and numerical simulations

### 4.1 Boundary Element Method (BEM) & Finite Element Method (FEM-COMSOL®)

The Boundary Element numerical method, which discretizes the boundaries only, is used to solve the resulting Helmholtz integral equation. The Green's function is in the form of a Hankel function of zero order. In BEM the element size must be at least five times smaller than the wavelength of interest. As it only meshes the boundaries, the resulting number of unknowns is reduced compared to FEM, however, the matrix equation is non-sparse.

COMSOL® multi-physics provides an interactive environment for modeling and solving acoustical problems based on the solution of partial differential equations (PDE) using the Finite Element Method (FEM) and assuming a cylindrical (line) source. Consequently it is suitable for predictions and investigations of sound propagation over rough surfaces. A two-dimensional finite element triangular mesh is generated to the fluid medium while the rough

surface is modeled as a rigid boundary with a similar profile. The other boundaries are modeled with a radiation boundary condition.

Figure 4 compares measured excess attenuation spectra with BEM and FEM (COMSOL®) predictions for periodic distribution of 13 triangular strips with centre-to-centre spacing of 6cm. Although the agreement between data and predictions is good, the predictions tend to overestimate the levels between 2 kHz and 3 kHz. The accuracy of BEM and FEM predictions can be improved by very fine meshing but this increases the computational resources required.

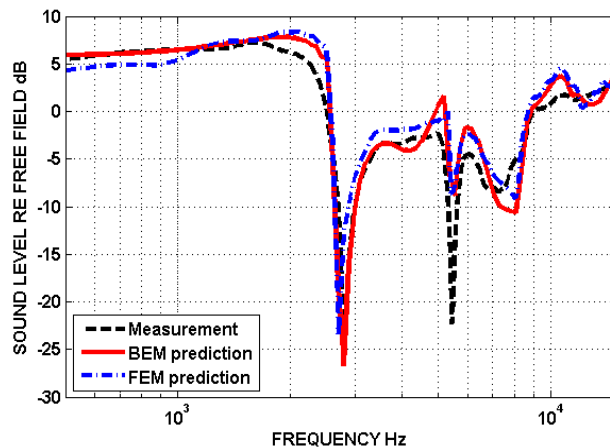


Figure 4: Comparison between MST predictions, BEM predictions and measured EA spectra over a glass sheet for 13 triangular strips with regular centre-to-centre spacing of 6cm.

### 4.2 Multiple Scattering Theory (MST)

Boulanger et al [8] extended Linton [9] formulation to provide a semi-analytical multiple scattering theory for the scattering of cylindrical acoustic waves by a finite array of semi-cylinders in a smooth hard surface. MST requires much less computational time and resources than either BEM or COMSOL (FEM). Figure 5 compares the measured excess attenuation spectra for a surface formed by semi-cylinders with a centre-to-centre 6 cm over a glass sheet with multiple scattering theory (MST) predictions. The predictions are in good agreement with the data; however, MST is valid only for semi-cylinders.

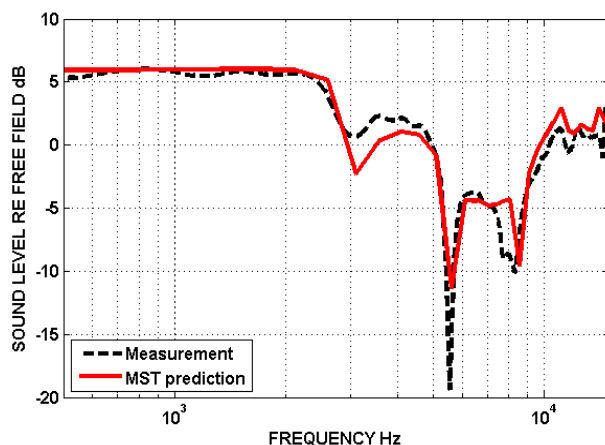


Figure 5: Comparison between MST predictions and measured EA spectra over a glass sheet for 11 semi-cylinders with regular centre-to-centre spacing of 6 cm.

## 5 Roughness-induced surface waves

Surface waves are generated by placing a point source very close to rough ground. A special case is diffraction from a periodically-rough boundary [10]. Surface waves exhibit exponential decay with height, cylindrical wavefront spreading and a slower wave speed than that in the unbounded fluid.

Figure 6(a) compares the measured EA spectra for two different random distributions of 13 triangular strips placed over MDF board with mean centre-to-centre spacing of 0.06 m with periodically spaced triangular strips having similar centre-to-centre spacing. Periodically spaced roughness elements show a stronger surface wave component than observed with randomly spaced elements having the same mean spacing. The example measured EA spectra for triangular strips with different spacings in figure 6(b) show that a smaller centre-to-centre spacing produces stronger surface waves.

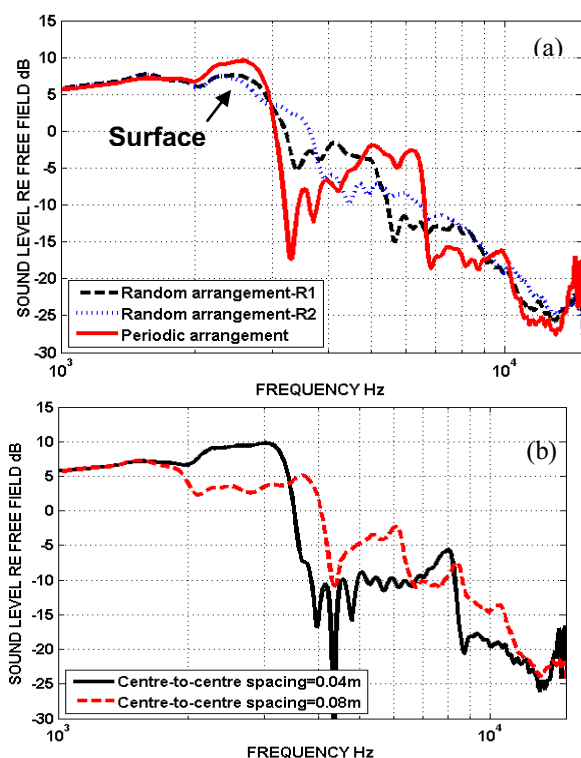


Figure 6(a): Measured excess attenuation spectra for source and receiver heights at 0.02 m separated by 0.7 m over triangular strips (a) random and periodic distributions with centre-to-centre spacing of 0.06 m (b) regularly-spaced with centre-to-centre spacings of 0.04 m and 0.08 m.

## 6 Effective Impedance models

### 6.1 Tolstoy's boss model for admittance

Tolstoy [1, 2] formulated boss models for predicting scattering of sound from surface roughness which is small as compared to wavelength. For oblique incidence at  $\alpha$  to the element axes and at azimuthal angle  $\varphi$ , the effective admittance of a surface containing 2-D roughness of arbitrary shape, is given by

$$\beta = -ik\varepsilon(\cos^2 \varphi - \sigma \cos^2 \alpha) \quad (1)$$

For grazing incidence normal to the periodically spaced roughness element axes,  $\alpha = \pi/2$  and  $\varphi=0$  hence the admittance is given by

$$\beta = -ik\varepsilon \quad (2)$$

The resulting admittance is purely imaginary. The scattering coefficient  $\varepsilon$  is defined as

$$\varepsilon = V \left( \frac{2s_2}{v_2} - 1 \right) \quad (3)$$

where  $V$  is cross-sectional scatterer area above the plane per unit length  $v_2 = 1 + 2\pi V s_2 / 3b$  is a scatterer interaction factor,  $s_2 = 0.5(1+K)$  is a shape factor,  $K$  is a hydrodynamic factor depending on steady flow around the scatterer of a given shape and  $b$  is the (mean) centre-to-centre spacing between roughness elements.

### 6.2 A heuristic surface impedance model

#### 6.2.1 A modified 'Tolstoy' component

Most of the work by Twersky [4, 5], Tolstoy [1, 2] and Medwin *et al* [6] considered closed packed roughness elements. Medwin *et al* [6] carried out measurements over both closed packed and regularly-spaced semi-cylinders but found that the agreement between predictions and data for the spaced roughness was poor. Moreover the measurements reported in sections 4 and 5 show that changing the centre-to-centre spacing between roughness elements of a given shape results in different EA spectra.

The only dependence on spacing in Eq.(2) is through  $v_2$ , and for a given cross-sectional shaped roughness and, for the laboratory data reported, the EA spectra predicted by eq.2 are not altered significantly if the centre-to-centre spacing is changed. On the other hand, the shape factor is assumed to have a constant value for any centre-to-centre spacing. Empirically, it has been found that agreement between predictions and data can be improved by making shape factor dependent on spacing.

The modified shape factor is given by

$$s_2 = 0.5 C_f (1+K) \quad (4)$$

where the empirically derived factor,  $C_f$ , is given by

$$C_f = 39b - 0.07 \quad (5).$$

#### 6.2.2 Effective layer component

Eq.(2) predicts a single EA maximum, whereas measured EA spectra show multiple distinct maxima. The impedance spectra deduced from EA data over a rough surface [11] show a resonances in the real and imaginary parts of impedance at the frequencies at which the second excess attenuation maximum occurs (see Figures 6 and 7). Essentially, the impedance spectra deduced above a rough surface resemble that for a hard-backed layer of porous material. Consequently, for the rough surface, a heuristically-introduced component is the impedance of a effective hard backed layer given by

$$Z_l = \coth(-ikd_e(1+0.04i)) \quad (6)$$

where  $d_e = (0.5+4h)b$  is the effective layer thickness and the complex wavenumber allows for viscous boundary layer effects.

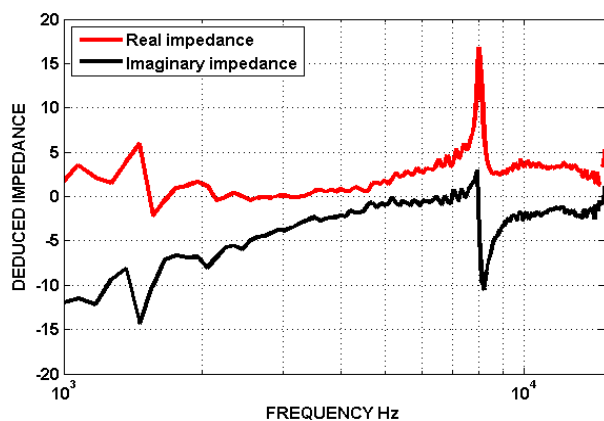


Figure 7: Impedance spectra for 15 triangular strips on a glass-sheet with centre-to-centre spacing of 4cm deduced from complex EA data.

The total effective impedance for a periodically-rough surface is given by

$$Z = 1 / \beta + Z_i \quad (7)$$

where  $\beta$  is given by Eqs. (2) – (5).

Figures 4 (a) and (b) compare measured EA spectra with those predicted by the original Tolstoy model (Eq.(2)) and Eq.(7) for periodically spaced triangular and semi-cylinders strips with centre-to-centre spacing of 3cm and 5cm respectively. The agreement between data and predictions using Eq.(7) is significantly better.

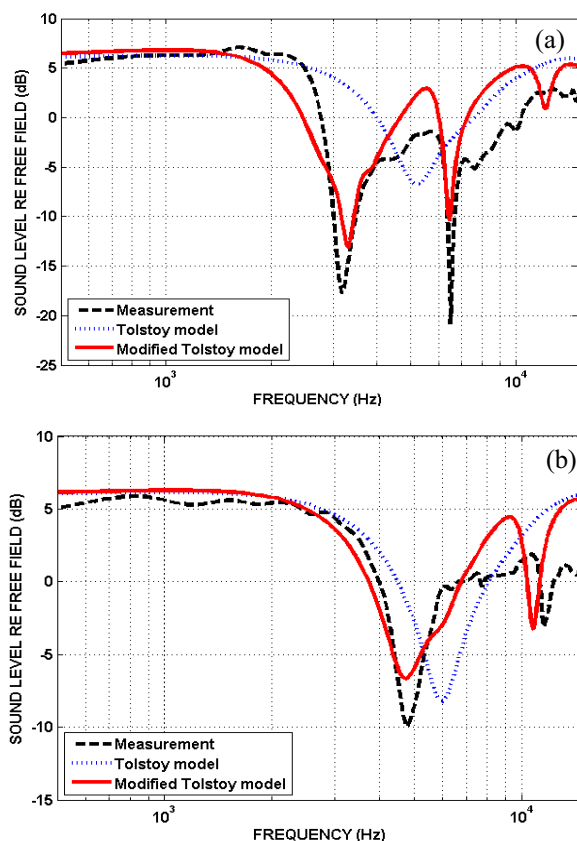


Figure 8: Comparison of Tolstoy and Modified Tolstoy predictions with measured EA spectra over a glass sheet by placing (a) 15 triangular strips with regular centre-to-centre spacing of 5cm (b) for 19 semi-cylinders with regular centre-to-centre spacing of 3cm.

## 7 Conclusion

The ground effect dips, corresponding to destructive interferences, observed in EA spectra measured over surfaces including randomly or periodically spaced roughness elements, which are small compared to the incident wavelengths, are at significantly lower frequencies than over a smooth hard surface for the same source-receiver geometry. Although a single broad EA maximum is observed for random spacing, multiple maxima appear in spectra measured over periodically spaced roughness. Also periodically spaced roughness elements are found to induce stronger surface wave components than randomly spaced roughness with the same mean spacing. An effective impedance model for a periodically-rough surface has been obtained by adding a modified Tolstoy component to the impedance of a hard-backed layer. Predictions of the resulting model show reasonably good agreement with data.

## Acknowledgments

The research leading to these results has received funding from the European Community's Seventh Framework Programme (FP7/2007-2013) under grant agreement n° 234306, collaborative project HOSANNA."

## References

- [1] I. Tolstoy, "Coherent sound scatter from a rough interface between arbitrary fluids with particular reference to roughness element shapes and corrugated surfaces", *J. Acoust. Soc. Am.* **72**, 960–972 (1982)
- [2] I. Tolstoy, "Smoothed boundary conditions, coherent low-frequency scatter and boundary modes", *J. Acoust. Soc. Am.* **72** 1–22 (1983)
- [3] M. A. Biot, "Generalized boundary condition for multiple scatter in acoustic reflection", *J. Acoust. Soc. Am.* **44**, 1616–1622 (1968)
- [4] V. Twersky, "On the non-specular reflection of plane waves of sound", *J. Acoust. Soc. Am.* **22**, 539–545 (1950)
- [5] V. Twersky, "On scattering and reflection of sound by rough surfaces", *J. Acoust. Soc. Am.* **29**, 209–225 (1957)
- [6] H. Medwin, G. L. D Spain, E. Childs and S. J. Hollis "Low-frequency grazing propagation over periodic steep-sloped rigid roughness elements", *J. Acoust. Soc. Am.* **76** 1174–90 (1984)
- [7] P. Boulanger, K. Attenborough, S. Taherzadeh, T. Waters-Fuller and K. M. Li, "Ground Effect Over Hard Rough Surfaces", *J. Acoust. Soc. Am.* **104** 1474–82 (1998)
- [8] P. Boulanger, K. Attenborough, Q. Qin and C. M. Linton, "Reflection of sound from random distributions of semi-cylinders on a hard plane: models and data", *J. Phys. D.* **38** 3480–3490 (2005)
- [9] C. M. Linton and P. A. Martin, "Multiple scattering by random configurations of circular cylinders: second-order corrections for the effective wave number", *J. Acoust. Soc. Am.* **117** 3413–23 (2005)
- [10] W. Luriks, L. Kelders and J. F. Allard, "Surface waves above gratings having a triangular profile", *Ultrasonics.* **36**, 865–871 (1998)
- [11] S. Taherzadeh and K. Attenborough "Deduction of ground impedance from measurements of excess attenuation spectra" *J. Acoust. Soc. Am.* **105** (3) 2039–2042 (1999)